JULY 1980

PPPL-1681
UC-20a

NUMERICAL SIMULATIONS ON ION ACOUSTIC DOUBLE LAYERS

BY

T. SATO AND H. OKUDA

PLASMA PHYSICS LABORATORY

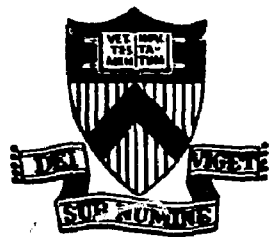

PRINCETON UNIVERSITY
PRINCETON, NEW JERSEY

This work was supported by the U.S. Department of Energy Contract No. DE-AC02-76-CHO 3073. Reproduction, translation, publication, use and disposal, in whole or in part, by or for the United States government is permitted.

Numerical Simulations on Ion Acoustic Double Layers

T. Sato* and H. Okuda

Plasma Physics Laboratory, Princeton University
Princeton, New Jersey 08544

(Received

A comprehensive numerical study of ion acoustic double layers has been performed for both periodic as well as for nonperiodic systems by means of one-dimensional particle simulations. For a nonperiodic system, an external battery and a resistance are used to model the magnetospheric convection potential and the ionospheric Pedersen resistance. It is found that the number of double layers and the associated potential buildup across the system increases with the system length. The potential jump $\Delta\phi_D$ across a single double layer is approximately $e\Delta\phi_D/T_e \approx 1$ and the distance between two consecutive double layers is typically 1000 Debye length where e and T_e are the electronic charge and temperature. There is little interaction among double layers and each double layer behaves almost independently from the others. The maximum increase of plasma energy through the enhanced resistance associated with double layer formation is found about 15% of the initial plasma energy for the parameters used in the simulations. The resistivity

takes its maximum value at the instance when the double layers are just formed and then drops to almost zero afterwards indicating the presence of a super conducting phase due to the formation of quasistable Bernstein-Green-Kruskal type equilibrium. The equilibrium is, however, unstable with respect to the emission of ion acoustic solitons and the double layers eventually decay as the solitons carry the energy away from the double layers propagating through a plasma toward the downstream direction.

I. INTRODUCTION

It is widely accepted that auroral electrons must be a product of parallel electric fields. In fact, there are several observations to support this idea [Frank and Ackerson, 1971; Evans, 1974; Arnoldy,et al., 1974; see, also, a review by Meng, 1978; Haerendel, et al., 1976; and Wescott,et al., 1976]. Among others, a double layer, or an electrostatic shock, is believed to be the most feasible and likely candidate for causing parallel electric fields [Mozer,et al., 1977].

Extensive analysis has also been made to study the conditions under which double layers can exist [Block, 1972, 1977; Knorr and Goertz, 1974; Swift, 1975, 1979; Kan, 1975]. All these theoretical works are, however, restricted to steady state double layers, so that they cannot answer an important question concerning the dynamical process of how a double layer is generated. It is very important in practical applications to study whether or not a double layer can be produced starting from realistic initial conditions in which, for example, no appreciable field-aligned potential drop exists. With respect to this question, several numerical simulations have been performed to demonstrate the formation of double layers in the presence of streaming electrons [Goertz and Joyce, 1975; DeGroot, et al., 1977]. Furthermore, there are several laboratory experiments which succeeded in observing formation of double layers [Torven and Babic, 1976; Torven and Anderson, 1979; Quon and Wong, 1976; Coakley and Hershkowitz, 1979; Iizuka,et al., 1979].

From these analytical, numerical, and laboratory investigations we may conclude that a double layer is a real existence. However, all these previous works concluded that double layers could not be realized if the electron streaming speed is less than the electron thermal speed. This conclusion, however, appears to contradict with the observations of double layers along auroral field lines. This is because it is unlikely that such a high speed electron drift exceeding the thermal speed exists along field lines before double layers are formed [Kindel and Kennel, 1971]. If, indeed, the large electron drift is required for the formation of double layers, we must look for some other mechanism to explain the observations of double layers along the auroral field lines. One of these mechanisms may be the anomalous resistivity which can cause large parallel electric fields to accelerate auroral electrons [Papadopoulos, 1977]. In this respect, it is interesting to note a historical controversy as to whether or not the anomalous resistivity plays the leading role in generating parallel electric fields [Block, 1975; Swift, 1975; Shawhan,et al., 1978; Papadopoulos, 1977]. In order to answer this question, it is obvious that one must study the time-dependent formation process of double layers since the steady state theory would not involve anomalous resistivity. A mechanism which interrupts the current must be involved in order to develop a dc potential jump in a current-carrying plasma in which no dc potential exists initially. Broadly speaking, it is reasonable to conclude that the formation of double layers is

associated with the generation of anomalous resistivity which interrupts the current causing the buildup of a dc potential.

In order to study the formation of double layers in the ion acoustic regime and whether or not the anomalous resistivity plays an essential role, extensive numerical simulations were recently carried out by the present authors [Sato and Okuda, 1980]. It was found that a double layer of the order of $e\Delta\phi_D/T_e \approx 1$ can be generated spontaneously even in the ion acoustic regime where the electron drift speed is less than the thermal speed when the system length is sufficiently long. In the previous paper [Sato and Okuda, 1980], a role of anomalous resistivity was suggested in order to explain the simulation results which required the length of the system to be more than several hunderd Debye length for the formation of double layers. Furthermore, it is worth mentioning that in the previous paper a periodic potential condition was adopted so that the boundary effects were eliminated in the ion acoustic double layers.

In the present paper, we wish to present results on numerical simulations on the development of ion acoustic double layers for the case in which the field-aligned current is connected to the magnetospheric convection. In addition, a resistance is inserted which models the ionospheric plasmas. The situation is schematically illustrated in Fig. 1.

II. NUMERICAL RESULTS

The initial plasma parameters employed in the simulations are the following: Electrons have a drifting Maxwellian distribution with $v_d = 0.6\ v_{eth}$ where v_d is the drift speed and v_{eth} is the thermal speed, whereas ions are a stationary Maxwellian with the temperature T_i. The temperature ratio $T_e/T_i = 20$, the mass ratio $m_i/m_e = 100$, and the plasma parameter $n\lambda_D = 100$ where λ_D is the electron Debye length. The time step Δt is taken to be $\omega_{pe}\,\Delta t = 0.2$ and the mesh size Δ is $\Delta = \lambda_D$.

A. Periodic Model

The previous simulations for a periodic case [Sato and Okuda, 1980] have shown that a double layer is formed when the system length L is 512 λ_D and 1024 λ_D but not when $L \leq 256\ \lambda_D$. The potential jump $\Delta\phi$ across the double layer (layer width is roughly 50 λ_D) was roughly 0.5 T_e/e for $L = 512\ \lambda_D$ and 1 T_e/e for $L = 1024\ \lambda_D$. It is interesting to observe what happens if the system length is further increased; whether a stronger double layer results or more than one double layer is formed. In order to answer this question, we performed a run with $L = 4096\ \lambda_D$ in which almost one million particles were used.

Figures 2 and 3 show the potential (top), electron density (middle) and ion density (bottom) distributions averaged over one plasma period at $\omega_{pe}t = 960$ and 720, respectively. From the potential profile at $\omega_{pe}t = 960$, it is evident that four similar double layers appeared in series instead of forming a single large layer when the system becomes longer than $1024\ \lambda_D$. Comparing each double layer with the previous run of $L = 1024\ \lambda_D$

[Fig. 1 of Sato and Okuda, 1980], it may be observed that the temporal development and the shape of each layer is almost identical with the previous one. From Fig. 3, it is clearly seen, in the density distributions, that there are indications of four large double layers with several more small fluctuations. In the potential profile the rightmost layer has already fully developed at this time, while the others are yet premature. At $\omega_{pe}t = 960$, the entire system is roughly equally divided into four segments by the double layers while the rightmost double layer which was dominant at $\omega_{pe}t = 720$ is already in a decaying phase.

From these results one can conclude several important observations. The fundamental length for an ion acoustic double layer to be formed is about 1000 λ_D. The potential jump $\Delta\phi$ associated with the layer is around 1 T_e/e and the double layer width is roughly 50 λ_D. At the upstream side, each double layer is characterized by the presence of a sharp negative potential spike whose width is about 10 λ_D. The location of a negative potential spike agrees with that of a pair of negative and positive ion density spikes suggesting the acceleration of ions due to the strong electric field at the location of potential spikes. As will be shown later, the potential profile of double layers decays as ion acoustic solitons emanate toward the downstream side of the double layer. Simultaneously, the density spikes become broader.

B. Bounded Model

We have shown that ion acoustic double layers can spontaneously be generated when a periodic boundary condition is assumed. It is natural to expect that the periodic boundary condition is not essential to form double layers in the simulations shown. This is because the system is long enough so that most of the electrons move only a fraction of the system by the time double layers are formed. Therefore, one can expect that ion acoustic double layers could easily be generated when the system is connected to an external source that drives the field-aligned current.

We have adopted a model in which the field-aligned current is connected to the magnetospheric convection field and is closed by the ionospheric Pedersen current as shown in Fig. 1(a). In order to simulate this system, an equivalent circuit model is developed as shown in Fig. 1(b). Initially, the plasma current $j_{\parallel 0}$ is given by $j_{\parallel 0} = \phi_o/R$ and the potential drop $\Delta\phi$ across the plasma system is set to be zero since the plasma is essentially collisionless and no resistivity exists. The current is assumed to be carried predominantly by electrons so that the current $j_{\parallel 0}$ is related to the electron drift velocity by $j_{\parallel 0} = -n_o e v_d$ where n_o is the initial electron density which is assumed to be uniform. As the ion acoustic waves are excited by the current, the electron drift velocity will decrease by the electric field fluctuations giving the momentum away to the ions. This process is associated with the generation of a nonlinear resistivity η. From the electric circuit of Fig. 1(b), the following relation is readily obtained:

$$\Delta\phi/\phi_o = \Delta j_{||}/ j_{||0} \qquad (1)$$

where $\Delta j_{||}$ is the current decrement due to the generated resistivity, hence, $\Delta\phi = \eta(j_{||0} - j_{||})$. In Eq. (1) ϕ_0 and $j_{||0}$ are given initially and $\Delta j_{||}$ can be measured at each time step of the simulation so that the potential difference across the system $\Delta\phi$ may be readily obtained from Eq. (1) at each time step. It is interesting to note that the ionospheric Pedersen resistivity R has nothing to do with the evolution of double layers; it merely determines the initial current intensity.

Simulations have been carried out for several cases in which the system length L is changed from 512 λ_D to 4096 λ_D and the applied potential $e\phi_o/T_e$ is changed from 10 to 200 with the other plasma parameters remaining the same as the previous periodic models. In order to avoid the buildup of charges near the boundary, particles leaving one end of the system are reinserted at the other end with the same speed. This may be considered a torus with a voltage gap.

Figure 4 shows a time evolution of the potential profile for the case where L = 1024 λ_D and $e\phi_o/T_e$ = 200. A clear indication of shock-like potential structure appears at $\omega_{pe}t$ = 540 whose amplitude grows in time. The structure is almost stationary with respect to the ion frame. This observation indicates that a double layer is not necessarily a phenomenon that is generated only when a potential difference across the system exceeds the electron thermal potential. At about $\omega_{pe}t$ = 900, the ion acoustic double layer reaches the

maximum amplitude where the net potential difference across the system becomes roughly $e\Delta\phi/T_e \simeq 0.7$ and the peak-to-peak potential difference $\Delta\phi_D$ at the shock position becomes as high as $e\Delta\phi_D/T_e \simeq 2$. In addition to the negative spike in front of the shock structure, note the development of spiky wave trains at the downstream side of the shock; the width of each spike is $10 \sim 15$ λ_D and its amplitude is $0.5 \sim 1$ T_e/e. These potential spikes propagate downward at the speed of the order of ion acoustic speed and as a result of propagation, the original shock structure is gradually destroyed. The spikes appear to be ion acoustic solitons from these observations. Therefore, we may conclude that the ion acoustic double layer is unstable with respect to the excitation of ion acoustic solitons. The observed life time of one double layer is roughly 500 ω_{pe} which is equal to the transit time of ion acoustic solitons to propagate across the double layer width ($\sim$ 50 λ_D) with the sound speed confirming the conclusion that the double layer decays as the solitons propagate out.

Shown in Fig. 5 are the potential structure and the density distributions of both ions and electrons at $t = 960$ ω_{pe}^{-1} where the double layer has fully developed. It is clear that the structure of the double layer is quite similar to that of the previous periodic models except for the presence of the net potential jump across the system.

Figure 6(a) shows the electron velocity distribution functions at $\omega_{pe}t = 960$ in the upstream region of the double layer averaged over a distance of $400 < x/\lambda_D < 550$, while the

distribution in the downstream region averaged over $550 \lesssim x/\lambda_D \lesssim 800$ is shown in Fig. 5(b). For comparison, corresponding velocity distributions at a much earlier time of $\omega_{pe}t = 60$ are also shown. In the upstream region, very little change is observed in the velocity distribution for $v \gtrsim v_{eth}$ while there is a substantial quasilinear-like deformation in the velocity range of $-v_{eth} \lesssim v \lesssim v_{eth}$ associated with the ion acoustic instability. The reduction of population in the range of $v < -v_{eth}$ is due to the deceleration of negative velocity electrons throu h the double layer. The decelerated electrons contribute partly in increasing the population in the range of $-v_{eth} \lesssim v \lesssim 0$. At the downstream region, on the other hand, it is clear that the streaming electrons with positive velocities are accelerated by the positive potential jump of the double layer, and therefore, a double-hump distribution is realized, where the energy of the accelerated electrons roughly correspond to the double layer potential jump. The increase of density for negative velocity may be due to the quasilinear-like diffusion. A rather symmetric distribution near the zero velocity may be due to reflection at the shock.

Since the prime objective of the present investigation is an application to auroral acceleration, it is important to study how much energy is extracted from the external energy reservoir to accelerate electrons through the formation of double layers. Shown in Fig. 7(a) are the total energy of the system in time for the cases where $L = 1024\ \lambda_D$ and $e\phi_o/T_e = 10$ (left side) and $L = 1024\ \lambda_D$ and $e\phi_o/T_e = 200$ (right side). It is clear, from

these observations, that, in spite of a large difference in the potential of the external source, the energy gain of the particles (electrons) from the external source is almost independent of the source potential. The energy gain is about 15% of the initial total energy. The total electric field energy and the average current are shown as a function of time in Figs. 7(b) and (c). It is clear that the field energy increases almost linearly with time until $\omega_{pe}t \simeq 720$ which is then followed by a burst-like increase. Correspondingly, the current undergoes a linear relaxation for $\omega_{pe}t \lesssim 720$ and then a drastic decrease takes place. The effective resistivity calculated from the slope of the linear relaxation corresponds to the normal ion acoustic anomalous resistivity, whereas the drastic decrease is associated with an "enhanced" resistivity [see, Sato and Okuda, 1980]. It is interesting to note that the appearance of the enhanced resistivity is associated with the formation phase of the double layer.

After the double layer is formed, plasma heating and current decrease are completely shut off and the resistivity disappears followed by the appearance of a "super" conductivity phase which appears after $\omega_{pe}t \gtrsim 1500$. From Fig. 7(c), it is observed that the current intensity relaxes to the initial level. Likewise, the total energy of the system has saturated suggesting the absence of resistivity in the system. Nevertheless, this superconducting phase is not the same as the initial quiescent uniform state. In this phase fairly large amplitude perturbations remain in both electron density and potential.

Particularly noted are the persistence of large amplitude density perturbations reaching about 20 ~ 30% of the background density. Notwithstanding, the resistivity in this phase is less than the classical resistivity due to thermal fluctuations. We believe the super conducting phase is associated with a new equilibrium state in which large fractions of particles are trapped via double layer potential structures. As mentioned earlier, this new equilibrium is not stable and the double layer decays in time by emitting ion acoustic solitons.

We shall next show results for the case in which the system length is $L = 512\ \lambda_D$. Shown in Fig. 8 are the profiles of the potential (a), electron density (b), and ion density (c) at two different times, $\omega_{pe}t = 1160$ (left) and $\omega_{pe} = 1400$ (right). In this case, the applied potential is $e\phi_o/T_e = 200$ and $\omega_{pe}t = 1160$ corresponds to the time when the double layer has fully developed. The potential difference across the system is $e\Delta\phi/T_e \simeq 0.4$ and the peak-to-peak potential difference at the shock position is $e\Delta\phi_D \simeq 1.8$. From Fig. 8(a), it is again seen that the double layer is destroyed by the emission of large amplitude ion acoustic solitons. It should also be remarked that the negative potential spike is formed at the shock front [see Fig. 8(a)] which persists even after the shock structure is destroyed.

Figure 9 shows the total energy (a), electric field energy (b), and the current density (c) for three different external potentials. The left, middle, and right columns correspond to $e\phi_o/T_e = 10$, 40, and 200, respectively. Comparing these three

cases, we again confirm there is no essential difference among these three as far as the total energy gain from the external source is concerned. The increase of total energy is about 22% of the initial plasma energy contained in the system with $L = 512\ \lambda_D$. In order to compare this energy gain with the previous case with $L = 1024\ \lambda_D$ where one full double layer is formed, we shall normalize this gain by the initial plasma energy contained in the system with $L = 1024\ \lambda_D$. Then it becomes 11% which is somewhat less than 15% of the previous case with $L = 1024\ \lambda_D$. This difference may be understood when we recall the conclusion derived from the periodic simulation that the unit system length for an independent double layer to be formed is about $1000\ \lambda_D$. We may conclude, therefore, that the energy gain from the external source per one full double layer is about 15% of the total plasma energy contained in the unit system length of $1000\ \lambda_D$.

Finally, we shall present the results of the case where the system length is $L = 4096\ \lambda_D$ and the applied potential is $e\phi_o/T_e = 200$. Figure 10 is the potential profile at $\omega_{pe}t = 960$ where several double layers are generated in cascades, some of them being already in decaying phase while others are newly-born layers. Remarkable is one large double layer located at the center of the system. The peak-to-peak potential difference reaches $e\Delta\phi_D/T_e \approx 2$ and the potential difference across the entire system is $e\Delta\phi/T_e \approx 1.5$. As was seen for the periodic model, each double layer develops more or less independently from the others. Because of this rather independent occurrence, the

total life time of double layers is prolonged compared with a shorter system in which fewer double layers are generated.

Figure 11(a), (b) shows the potential and density structures at $t = 1800\ \omega_{pe}$ where the amplitudes of double layers decreased considerably. It is interesting to observe that while large density spikes persist at the locations of double layers, the corresponding potential structure is much smoother and no apparent spikes persist. At this stage, the plasma is at the super conducting phase and no anomalous resistivity exists consistent with the absence of potential double layers. In this respect, large density discontinuities seen in Fig. 11(b) do not necessarily guarantee the presence of double layers and there is no linear relation such as $e\phi/T_e = \delta n/n$ in this highly nonlinear phase.

Table I summarizes the potential jump across the system $e\Delta\phi/T_e$ and the peak-to-peak drop $e\Delta\phi_D/T_e$ for $L = 512\ \lambda_D$, $1024\ \lambda_D$, and $4096\ \lambda_D$. From these results, we conclude that the total potential difference across the system becomes larger as the system becomes longer. Since each double layer behaves almost independently from the others, the life-time of double layers of the entire system becomes longer as the system is increased. This is because, as seen in Fig. 9, some double layers are growing while others are already decaying which have no phase information with each other.

III. DISCUSSIONS AND CONCLUSIONS

By means of extensive numerical studies of an ion acoustic instability, it is confirmed that an ion acoustic instability results in ion acoustic double layers if the system is sufficiently long, irrespective of whether the system is periodic or bounded. The results from the simulations have shown that the ion acoustic double layers are generally formed in series with the average spacing of 1000 λ_D between two layers. A double layer is characterized by the presence of a negative potential spike in front of the layer in addition to the monotonic positive jump in potential. The peak-to-peak potential is roughly $2\ T_e/e$ and the typical width of the potential jump is 50 λ_D. Each double layer decays in time as a result of the propagation of ion acoustic solitons and the life time is equal to a transit time of solitons across a double layer. There is little interaction among different double layers. The energy that one double layer can gain from the external source is roughly 15% of the total energy contained in 1000 Debye length irrespective of the magnitude of the external potential.

An important conclusion deduced from the bounded model is that the total potential difference across the system increases with the system size. Furthermore, for a very long system in which many double layers are present, it is natural to expect that double layers always exist which are located more or less randomly throughout the entire system. This observation is essential when applied to the auroral problem, because a potential jump much larger than the electron thermal energy may be expected to arise. The observational fact that a "super"

conducting phase follows the double layer formation also provides a challenging problem in nonlinear plasma physics although it is clearly related to the BGK type equilibrium.

In the present paper we have adopted a model in which the field-aligned current is driven by a twin-convection cell in the magnetospheric equator. Actually, there may be other current sources [Sato and Iijima, 1979; Hasegawa and Sato, 1979]. As discussed in the paper by Sato and Iijima, it is most likely that the Region 1 field-aligned current pairs are driven by the convective plasma motion in the magnetosphere. Furthermore, a recent global simulation of auroral arc formation [Miura and Sato, 1980], based on Sato's ionosphere-magnetosphere feedback instability [Sato, 1978], has shown that auroral arcs in the evening sector occur in the location of upward Region 1 current. Therefore, the present model connected to magnetospheric plasma convection may be meaningful. It is, of course, required that simulation models based on other field-aligned current sources be studied in the future.

Before concluding this paper, we shall present two more diagnostics which would help elucidate the generation mechanism of double layers. One of them is a power frequency spectrum of the electric field average over $0 \lesssim t \lesssim 800\ \omega_{pe}$ at various locations. The sample employed in this analysis is the periodic case with $L = 1024\ \lambda_D$ [Sato and Okuda, 1980]. Figure 12 shows power spectra measured at six different locations of $x/\lambda_D = 560, 570, 580, 590, 600, 610$, where the first four are in the upstream region of the double layer while $x/\lambda_D = 600$ is

almost on the negative spike and the last location is in the double layer after the negative spike. The largest two symmetric peaks observed at x/λ_D = 560, 570, and 580 represent the linearly most unstable ion acoustic mode. Approaching to the shock front, a different ion acoustic mode emerges at about x/λ_D = 580. The frequency appears to be bifurcated from the frequency of original instability toward lower frequency and the amplitude of the new mode grows much larger than the original one, by a factor of 10. At x/λ_D = 580, the frequency of the new mode is slightly less than that of the original ion acoustic instability and the amplitude is somewhat less than that of the original mode. At x/λ_D = 590, however, the new mode dominates the original mode. At x/λ_D = 600 whose location is very close to the shock front, the amplitude of the new mode is about one order of magnitude larger than that of the original mode and the frequency is substantially lower. At x/λ_D = 610, which is inside the layer, the frequency reduced to almost zero. The reason that the amplitude is small is because the measurement was done at a location where the negative spike goes back to zero before monotonic increase associated with the double layers begins. The frequency measurements at the locations after the double layer indicate the absence of new low frequency mode and the original ion acoustic instability again becomes dominant. Figure 13 shows the time history of the electric field at the same locations shown in Fig. 12. It is remarkable to observe how the new low frequency mode propagates from left to right with the wavelength much longer than the original most unstable ion

acoustic instability. For example, the new mode begins to appear at $\omega_{pe} \simeq 400$ at $x/\lambda_D = 580$, and propagates downstream at roughly the sound speed while the amplitude is amplified. That is, the new mode appears to grow convectively, while the frequency is lower than the original unstable mode. The convective speed is about 0.1 v_{eth} which is the ion acoustic speed.

While we believe the generation of new modes and hence the formation of double layers is due to the acceleration of electrons associated with the ion acoustic anomalous resistivity [Sato and Okuda, 1980], one cannot rule out other possibilities at this moment. One such possibility is the decay of the unstable modes associated with the ion acoustic instability to the low frequency mode by mode coupling. An instability of a BGK wave is also another potential candidate. Further investigation on this matter will be reported.

ACKNOWLEDGMENTS

We wish to thank Dr. A. Hasegawa, Dr. H. Ikeji, Dr. T. O'Neil, and Dr. Yamada for their interest in this work and useful discussions.

This work was supported by United States Department of Energy Contract No. DE-AC02-76-CH03073.

TABLE I

Potential jump across double layer ($e\,\Delta\phi_D/T_e$) and across the system ($e\,\Delta\phi/T_e$).

	$L = \_\_ \lambda_D$	$L = 1024\ \lambda_D$	$L = 4096\ \lambda_D$
$e\,\Delta\phi_D/T_e$	1.8	2.0	2.0
$e\,\Delta\phi/T_e$	0.4	0.8	1.6

REFERENCES

*Permanent Address: Geophysics Research Laboratory, University of Tokyo, Tokyo 113, Japan.

Arnoldy, R. L., P. B. Lewis, and P. O. Issacson, Field-aligned auroral electron fluxes, J. Geophys. Res., 79, 4208, 1974.

Block, L. P., Potential double layers in the ionosphere, Cosmic Electrodynamics, 3, 349, 1972.

Block, L. P., Double layers, Physics of the hot plasma in the magnetosphere, edited by B. Hultquist and L. Stenflo, Plenum Pub. Co., New York, p. 229, 1975.

Block, L. P., A double layer review, Astro. Space Sci., 55, 59, 1977.

Coakley, P. and N. Hershkowitz, Laboratory double layers, Phys. Fluids, 22, 1171, 1979.

DeGroot, J. S., C. Barnes, A. E. Walstead, and O. Buneman, Localized structures and anomalous dc resistivity, Phys. Rev. Lett., 38, 1283, 1977.

Frank, L. A. and K. L. Ackerson, Observations of changed particle precipitation into the auroral zone, J. Geophys. Res., 76, 3612, 1971.

Goertz, C. K. and G. Joyce, Numerical simulation of the plasma double layer, Astrophys. Space Sci., 32, 165, 1975.

Haerendel, G., E. Rieger, A. Valenzuela, H. Föppl, H. C. Stenback-Nielsen, and E. M. Wescott, First observation of electrostatic acceleration of barium ions into the magnetosphere, in European Programmes on Sounding-Rocket and Balloon Research in the Auroral Zone, Space Agency Report, ESA-SP115, Neuilly, France, August, 1976.

Iizuka, S., K. Saeki, N. Sato, and Y. Hatta, Buneman instability, Pierce instability, and double-layer formation in a collisionless plasma, Phys. Rev. Lett., 43, 1404, 1979.

Kan, J. R., Energization of auroral electrons by electrostatic shock waves, J. Geophys. Res., 80, 2089, 1975.

Kindel, J. M. and C. F. Kennel, Topside current instabilities, J. Geophys. Res., 76, 3055, 1971.

Knorr, G. and C. Goertz, Existence and stability of strong potential double layers, Astrophys. Space Sci., 31, 209, 1974.

Meng, C.-I., Electron precipitations and polar auroras, Space Sci. Rev., 22, 223, 1978.

Miura, A. and T. Sato, Numerical simulation of global formation of auroral arcs, J. Geophys. Res., 85, 73, 1980.

Mozer, F. S., C. W. Carlson, M. K. Hudson, R. B. Torbert, B. Parady, J. Yatteau, and M. C. Kelley, Observations of paired electrostatic shocks in the polar magnetosphere, Phys. Rev. Lett., 38, 292, 1977.

Papadopoulos, K., A review of anomalous resistivity for the ionosphere, Rev. Geophys. Space Phys., 15, 113, 1977.

Quon, B. H. and A. Y. Wong, Formation of potential double layers in plasmas, Phys. Rev. Lett., 37, 1393, 1976.

Sato, T., A theory of quiet auroral arcs, J. Geophys. Res., 83, 1042, 1978.

Sato, T. and T. Iijima, Primary sources of large-scale Birkeland currents, Space Sci. Rev., 24, 347, 1979.

Sato, T. and H. Okuda, Ion acoustic double layers, Phys. Rev. Lett., 44, 740, 1980.

Shawhan, S. D., C-G. Fälthammar, and L. P. Block, On the nature of large auroral zone electric fields at 1-h_E altitutdes, J. Geophys. Res., 83, 1049, 1978.

Torven, S. and M. Babic, Current limitation in low pressure mercury arcs, Proc. Fourth Int. Conf. on Gas Discharges, Swansea, p. 323, 1976.

Torven, S. and D. Anderson, Observations of electric double layers in a magnetized plasma column, J. Phys., 12, 717, 1979.

Wescott, E. M., H. C. Stenback-Nielsen, T. J. Hallinan, and T. N. Davis, The skylab barium plasma injection experiments: 2. Evidence for a double layer, J. Geophys. Res., 81, 4495, 1976.

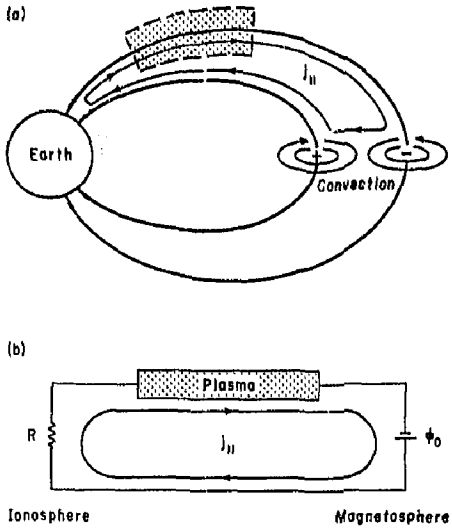

(PPPL-802058)

Fig. 1. A model of coupled magnetosphere-ionosphere systems (a) and its equivalent ciruit representation employed in the present simulation (b). Field-aligned current $J_{\parallel}$ is assumed to be driven by the magnetospheric convection.

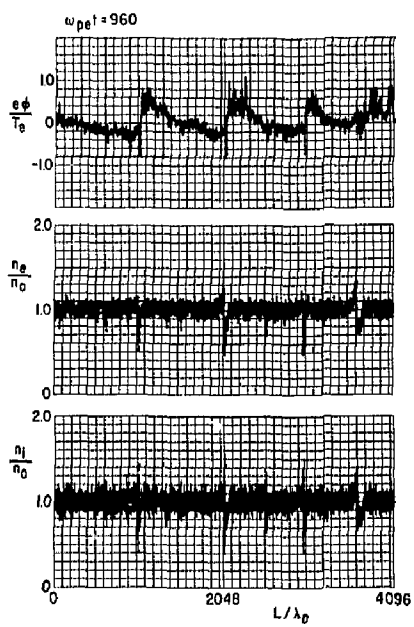

(PPPL-792493)

Fig. 2. Potential (top), electron density (middle), and ion density (bottom) profiles at $\omega_{pe}t = 960$ for the periodic model with L (system length) = $4096\lambda_D$.

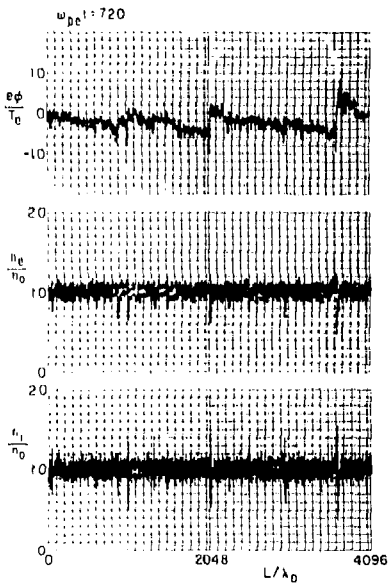

(PPPL-792492)

Fig. 3. Potential (top), electron density (middle), and ion density (bottom) profiles at $\omega_{pe}t = 720$ for the periodic model with $L = 4096\ \lambda_D$.

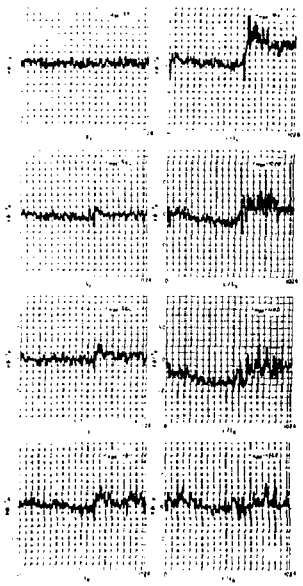

(PPPL-792356)

Fig. 4. A time evolution of a potential double layer for the bounded model with $L = 1024\lambda_D$ and $e\phi_o/T_e = 200$. It is interesting to observe that a shock-like structure is maintained even at the very beginning of its occurrence and its amplitude grows in time. Note also that the double layer is unstable with respect to the excitation of ion acoustic solitons.

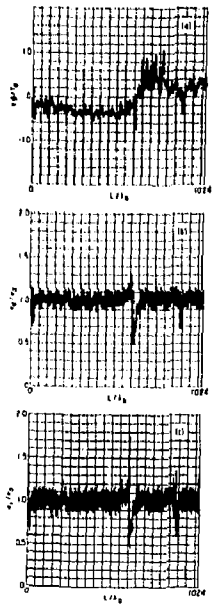

(PPPL-792359)
Fig. 5. The potential structure (a) and the density distributions of electrons (b) and ions (c); the same case as in Fig. 4.

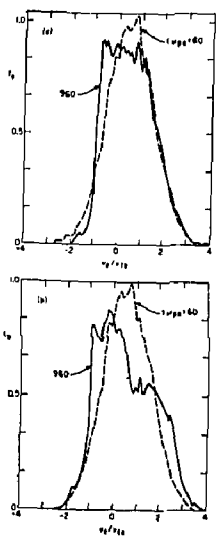

(PPPL-792358)
Fig. 6. Velocity distributions of electrons in the upstream region averaged over a distance of $450 \leq x/\lambda_D \leq 550$ (a) and in the downstream region averaged over $650 \leq x/\lambda_D \leq 800$ (b) for the same case as in Fig. 4; the solid lines stand for $\omega_{pe}\, t = 960$ and the dashed lines for $\omega_{pe}\, t = 60$.

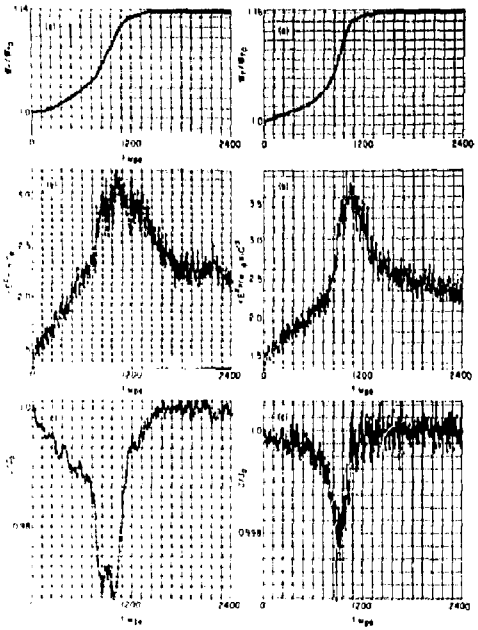

(PPPL-792362)
Fig. 7. Temporal changes of the total energy of the system (a), the total electric field energy (b), and the average current (c) for the same case as in Fig. 4 (right side) and for the case where $L = 1024\lambda_D$ and $e\phi_o/T_e = 10$ (left side).

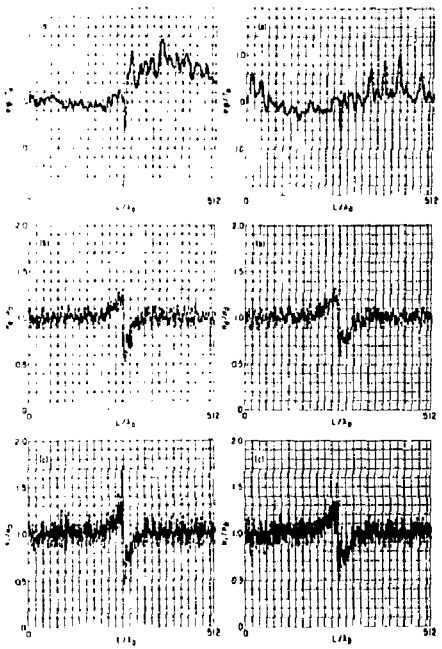

(PPPL-792361)
Fig. 8. The potential structures (a), the density distributions of electrons (b), and ions (c) at ω_{pe} t = 1160 (left) and ω_{pe} t = 1400 (right) for $L = 512\lambda_D$ and $e\phi_o/T_e = 200$.

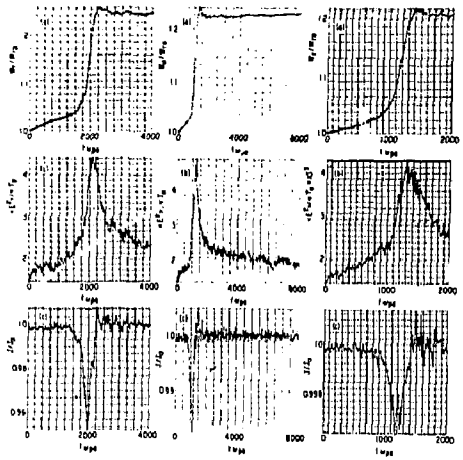

(PPPL-792353)

Fig. 9. Temporal evolution of the total energy in the system (a), the total electric field energy (b), and the average current (c) for the same case as in Fig. 8 (left), for the case where L = $516\lambda_D$ and $e\phi_o/T_e$ = 40 (middle) and for the case where L = $516\lambda_D$ and $e\phi_o/T_e$ = 10.

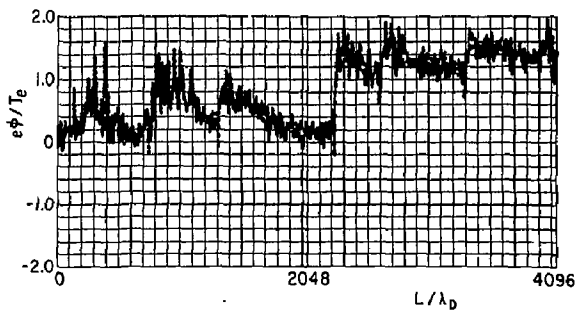

(PPPL-802059)

Fig. 10. The potential profile at $\omega_{pe}t$ = 960 for the case where $L = 4096\lambda_D$ and $e\phi_o/T_e$ = 200. Note a development of larger total potential difference compared with the cases with smaller system length.

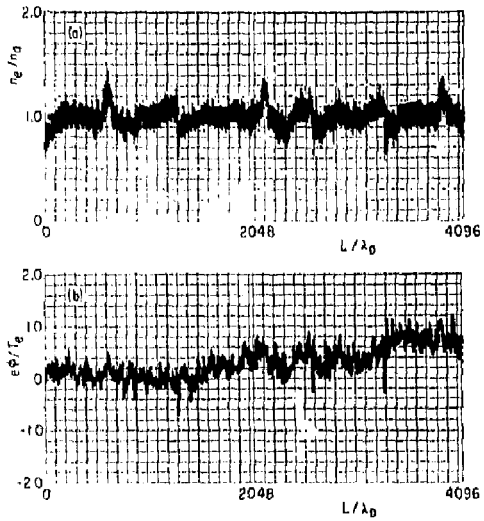

(PPPL-802090)

Fig. 11. The potential (a) and density (b) structures at ω_{pe} t = 1800 for the same case as in Fig. 10. It is interesting to observe that while the amplitude of double layers has decreased considerably, large density spikes and jumps persist at the locations of double layers. More interesting is that at this stage the plasma is at the super conducting phase.

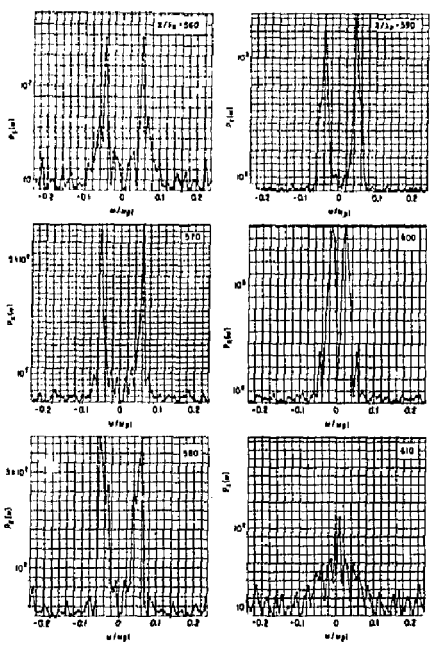

(PPPL-802055)

Fig. 12. Power frequency spectra of the electric field averaged over $0 \leq \omega_{pe}\, t \leq 800$ at six different places (x/λ_D) for the periodic case with $L = 1024\lambda_D$ [see, Sato and Okuda, 1980]. The first four locations are in the upstream region, while $x/\lambda_D = 600$ is almost on the negative spike and the last is the double layer just after the negative spike. Note a generation of new low frequency modes.

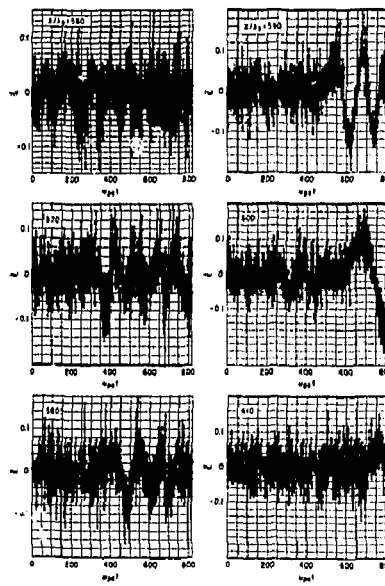

(PPPL-802067)

Fig. 13. The time history of the electric field at the same locations as in Fig. 12. The new low frequency mode is observed to be convectively amplified, the convection speed being the ion acoustic speed.